Models of Synchronized Hippocampal Bursts in the Presence of Inhibition.

I. Single Population Events

ROGER D. TRAUB, RICHARD MILES, AND ROBERT K. S. WONG

IBM T. J. Watson Research Center, Yorktown Heights, 10598; and Department of Neurology, Columbia University College of Physicians and Surgeons, New York, New York 10032

SUMMARY AND CONCLUSIONS

1. We constructed model networks with 520 or 1,020 cells intended to represent the CA3 region of the hippocampus. Model neurons were simulated in enough detail to reproduce intrinsic bursting and the electrotonic flow of currents along dendritic cables. Neurons exerted either excitatory or inhibitory postsynaptic actions on other cells. The network models were simulated with different levels of excitatory and inhibitory synaptic strengths in order to study epileptic and other interesting collective behaviors in the system.

2. Excitatory synapses between neurons in the network were powerful enough so that burst firing in a presynaptic neuron would evoke bursting in its connected cells. Since orthodromic or antidromic stimulation evokes both a fast and a slow phase of inhibition, two types of inhibitory cells were simulated. The properties of these inhibitory cells were modeled to resemble those of two types of inhibitory cells characterized by dual intracellular recordings in the slice preparation.

3. With fast inhibition totally blocked, a stimulus to a single cell lead to a synchronized population burst. Thus the principles of our epileptic synchronization model, developed earlier, apply even when slow inhibitory postsynaptic potentials (IPSPs) are present, as apparently occurs in the epileptic hippocampal slice. The model performs in this way because bursting can propagate through several generations in the network before slow inhibition builds up enough to

block burst propagation. This can occur, however, only if connectivity is sufficiently large. With very low connection densities, slow IPSPs will prevent the development of full synchronization.

4. We performed multiple simulations in which the fast inhibitory conductance strength was kept fixed at various levels while the strength of the excitatory synapses was varied. In each simulation, we stimulated either one or four cells. For each level of inhibition, the peak number of cells bursting depended sensitively on excitatory synaptic strength, showing a sudden increase as this strength reached a critical level. The critical excitation, which depended on the level of inhibition, corresponded to the level at which bursting can propagate from cell to cell at the particular level of inhibition.

5. We performed an analogous series of simulations in which the strength of excitatory synapses was held constant while the strength of fast inhibitory synapses was varied, stimulating a single neuron in each case. These simulations correspond to experiments that have been done in the hippocampal slice as low doses of picrotoxin are washed into a slice, gradually abolishing fast inhibition. At least some neurons in the model (as much as 4% of the population) burst in response to this minimal stimulus even with large inhibitory strengths. This occurs because some cells receive an excitatory input before they are inhibited.

6. As fast inhibition was reduced, the number of cells bursting started to increase suddenly as cell-to-cell propagation of bursting increased. The inflection point in the

peak number bursting versus inhibitory strength curve occurred at a level of inhibition larger than expected based on calculations with three-cell networks (i.e., with 1 neuron excited and inhibited by 1 other neuron, respectively). The reason for this is that multicellular interactions become important at levels of inhibition near the threshold for developing a large population response. Plotting the number of cells bursting as a function of time, we observed that with intermediate levels of inhibition, synchronization was incomplete, of prolonged latency, and not sharp. As inhibition was reduced further, synchronization increased, shortened in latency, and sharpened.

7. To better understand the cellular basis for the different responses of the system as inhibition was diminished, we compared the responses of individual cells with the population response. One sequence of experimental cellular responses observed with diminishing inhibition is an excitatory postsynaptic potential (EPSP), a pair of EPSPs, an EPSP followed by a burst, and an EPSP merging into a burst. We also observed this sequence in our model. We correlated the response of the single cell with the activities of its synaptic precursors: the single EPSP corresponded to a burst in 1 of its 14 precursors, the double EPSP to slightly asynchronous bursts in two precursors, etc. Thus the differing cellular reactions reflect increasing propagation of bursting over more and longer paths as inhibition is blocked.

8. Our hippocampal slice model accounts not only for epileptic synchronization with fast inhibition totally blocked, but also for a variety of collective phenomena occurring when at least some fast inhibition is intact.

INTRODUCTION

We have previously developed a model of the epileptic hippocampal slice (43, 46). While many features have been added to this model [e.g., electric field effects (42) and axonal conduction delays (44)], the cardinal ideas have remained: the ability of CA3 pyramidal neurons to develop intrinsic bursts (40, 51, 52), the existence of a network of sparse, putatively random and powerful excitatory synaptic interconnections (22, 26), and the ability of bursting to propagate from

cell to cell (24, 26). Propagation of bursting from cell to cell can occur, since *1*) at least some excitatory synapses are powerful enough to allow faithful burst-to-burst transmission (24, 26) and *2*) many convulsant agents block or at least diminish one form of synaptic inhibition that normally appears to limit burst propagation (9, 50).

In this paper, we address three main issues. First, there is a slowly developing and decaying form of synaptic inhibition in the CA3 region (18, 38). Data from CA1 and CA3 suggest that this slow inhibition is K^+-dependent and is resistant to the effects of convulsant agents such as picrotoxin (2, 18, 30, 38). While it has not been shown directly that slow inhibitory postsynaptic potentials (IPSPs) are activated through local axon collaterals (as opposed to feedforward effects from orthodromic stimuli), it is the case that an ethyleneglycol-bis(β-aminoethylether)-N,N'-tetraacetic acid-resistant hyperpolarization occurs during penicillin-induced synchronized bursts (12, 35), and this hyperpolarization is likely to result from a slow IPSP, at least in part. We therefore ask whether our model of synchronization functions in the case where there are inhibitory neurons, which *1*) are activated by pyramidal neurons and *2*) which produce widespread slow IPSPs. We answer this question in the affirmative, provided that the excitatory connectivity is not too sparse.

The second issue concerns the changing cellular interactions, and the population correlates, as "fast" inhibition is progressively blocked with picrotoxin (PTX). Thus polysynaptic excitatory pathways appear to be progressively "uncovered" as PTX exerts its effects, in the sense that two cells, that initially appear synaptically uncoupled, begin to interact more and more strongly. (The interaction is generally in one direction only.) An experimentally observed example of such changing interactions is the following: a train of action potentials in cell A appears first to have no effect on cell B, then produces an excitatory postsynaptic potential (EPSP) in B, then a series of two EPSPs, then an EPSP followed by a burst, and then an EPSP merging into a burst (the latency to the burst decreasing progressively) (28). We asked if a randomly connected network of excitatory and inhibitory neurons could generate a sim-

ilar sequence of events as a single parameter (fast inhibitory conductance strength) was varied, all other parameters, including slow inhibitory conductance strength, remaining constant. This indeed turns out to be the case. That it should be the case is far from obvious, since one can imagine that as inhibition is reduced, there would be a sudden jump from no propagation of activity from cell A to a situation where there is propagation from A to all the rest of the population, producing a synchronized burst (24). However, in networks not too densely connected, there is a range of inhibition in which significant activity can propagate through the system without causing a synchronized burst, this activity producing a series of EPSPs, EPSP/IPSP mixtures, or bursts in selected other cells.

The third issue is the following. Given that the network behavior appears to agree closely with certain experiments, we wished to investigate the effects of varying both excitatory and inhibitory synaptic strengths. There are two reasons for doing this. First, synchronized bursts are known to occur in situations where synaptic inhibition is not totally blocked, or may even be enhanced (5, 10, 32, 47, 49). Examples include 4-aminopyridine [which may augment all types of synaptic transmission (5, 33)], high K^+ [which changes the reversal potential of IPSPs—including Cl^- IPSPs—in a depolarizing direction (21)], and, more speculatively, interictal spikes in human epileptic patients (54), where it seems unlikely that inhibition would be totally blocked. We show that if excitatory synapses are powerful enough, considerable synchronization can occur over a large range of inhibitory strengths. The resulting synaptic inputs to particular cells are mixtures of excitation and inhibition, consistent with observations of Rutecki et al. in high K^+ media (32). The second reason concerns our interest in two related aspects of the system's behavior that may be of biological importance: first, the extent to which a burst in a single neuron can influence the firing of other neurons in the population, and second, the tendency of different neurons either to fire in phase with each other or to develop simultaneous synaptic potentials. If simultaneous firing is pronounced but not complete, we may speak of

"partial synchronization." We wish to analyze the specific parameters that influence these behaviors.

All the simulations reported here concern networks of neurons that begin in a resting state, and for which all synapses of a given type have the same strength. This idealization simplifies the analysis, but, of course, neurons in the hippocampal slice are probably never truly at rest, nor are different synapses likely to have identical properties. In the next paper in this series we analyze partially synchronized events in a system with ongoing activity that continues over many seconds; in that case, the system is never truly at rest and several of the model parameters have values scattered over an appropriate range.

METHODS

Overall structure of array

We simulated networks with 500 excitatory neurons ("e-cells") and 20 inhibitory neurons ("i-cells"), or with 1,000 e-cells and 20 i-cells. It is generally believed that there are many more e-cells in hippocampus than i-cells, although the exact ratio is not known to our knowledge. In the CA1 region, estimates of 0.5–5.8% have been obtained for the fraction of repetitively firing neurons (19, 34). In CA1, repetitively firing neurons have been shown to produce inhibitory postsynaptic potentials (19). The e-cells were arranged in either a 10 × 50 or 20 × 50 array, and the i-cells were scattered across the array, sometimes extending beyond the boundaries of the e-cells. The spatial location of the cells was important only for determining conduction delays, since all the connectivity parameters were random (see below). We specify the position of cells by the pair of indices (k, l). For an e-cell, $1 \le k \le 10$ or 20, and $1 \le l \le 50$.

Neuron types and intrinsic properties

In these simulations, we modeled neurons with both excitatory and inhibitory postsynaptic actions. All e-cells have bursting characteristics, consistent with physiological data from the CA3 region. In simulating i-cells, we wished to account for the observation that stimulation of fiber pathways evokes synaptic responses with a fast and a slow phase of inhibition in CA3 cells. It is not completely clear whether these components are initiated by two separate types of inhibitory cells. However, in simultaneous intracellular recordings from the hippocampal slice preparation, inhibitory cells with two different firing patterns have been observed (see Ref. 25, which also contains a

A

B

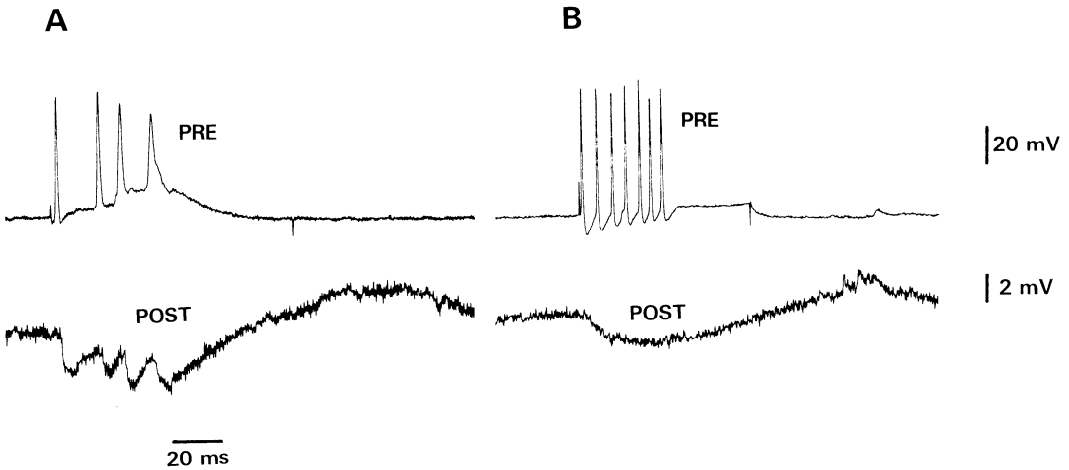PRE

PRE

| 20 mV

| 2 mV

POST

POST

———
20 ms

FIG. 1.   Two types of inhibitory synaptic interaction. Data obtained from simultaneous intracellular recordings in the CA3 region of the hippocampal slice. *A*:   cells which discharge action potentials followed by afterdepolarizations elicited discrete unitary IPSPs. Synaptic events follow each presynaptic action potential at short latency and have a rapid time course. *B*:   cells which discharge action potentials followed by prominent afterhyperpolarizations evoke a slowly developing synaptic inhibition in postsynaptic neurons.

description of experimental procedures). Neurons with a burst firing pattern can evoke a rapidly rising IPSP, which decays with time constant similar to that of the postsynaptic membrane (Fig. 1*A*). Unitary events follow each presynaptic action potential, with latency <1 ms, at frequencies up to 80 Hz; such unitary events are blocked by the γ-aminobutyric acid (GABA) antagonist picrotoxin (28). Another type of inhibitory cell fires repetitively with action potentials followed by a prominent afterhyperpolarization (19, 25). A slow hyperpolarization, in which unitary events are difficult to resolve, is evoked in connected cells by a train of presynaptic action potentials (Fig. 1*B*). In the absence of more complete data, inhibitory synaptic interactions were modeled to resemble these two cell types (Fig. 1). Half of the inhibitory cells were burst firing and half were repetitively firing. We note that hippocampal neurons with pyramidal morphology have been found that take up GABA (14) or that react with anti-GABA antibodies (12), although Ribak, Vaughn, and Saito (31) did not find glutamic acid decarboxylase staining of typical pyramidal neurons.

The method of simulating bursting neurons was as in previous publications (40, 43). Each bursting neuron contains 28 compartments (one for the soma, 27 for the dendrites), with burst-generating sites at the soma and in one apical dendritic compartment. At each bursting site, there are five active ionic conductances: Na^+, delayed rectifier K^+, Ca^{2+}, Ca^{2+}-dependent K^+ (3, 15, 51), and the M-current K^+ conductance (1, 13). All compartments contain a membrane capacitance and voltage-independent leakage conductance, and the compartments are interconnected by resistors

corresponding to the resistivity of the intracellular medium. Specific membrane resistivity (R_m) was 10,000 $\Omega \cdot cm^2$, specific membrane capacitance (C_m) was 3.0 $\mu F/cm^2$ [in the range observed by Turner and Schwartzkroin (48)], and internal cytoplasmic resistivity (R_i) was 100 $\Omega \cdot cm$. The apical dendrites are 1.0 space constant and the basilar dendrites 0.8 space constants, respectively, in electrotonic length. Each bursting cell has an input resistance of 32 MΩ, and the input resistance of the apical branch with the bursting site is 90 MΩ. The equations describing each neuron are as in Ref. 40, with the M-current as in Ref. 43 and $\bar{g}_M = 0.1 \times \bar{g}_K$.

Data on the intrinsic properties of repetitively firing i-cells are limited. We therefore did not construct ab initio the electrotonic properties of these neurons, but rather converted our bursting model neuron into a repetitively firing model. This was done by removing the calcium conductance and calcium-dependent conductances and by altering the voltage-dependent g_K. Thus, in bursting neurons, $g_K = \bar{g}_K n^4 y$, where n is analogous to Hodgkin-Huxley n and y is a time- and voltage-dependent inactivation variable (40). In repetitively firing neurons, y is kept identically equal to 1 (Fig. 2). In repetitively firing model neurons, there is also no M-current.

Synaptic interactions

Each kind of cell sends an output toward its connected followers if the soma potential is >20 mV and no output has been sent for 3 ms (corresponding to a refractory period for interconnecting axons). The signal arrives at the various postsynaptic sites at different times that de-

A

PRE | 20 mV

| 2 mV

POST
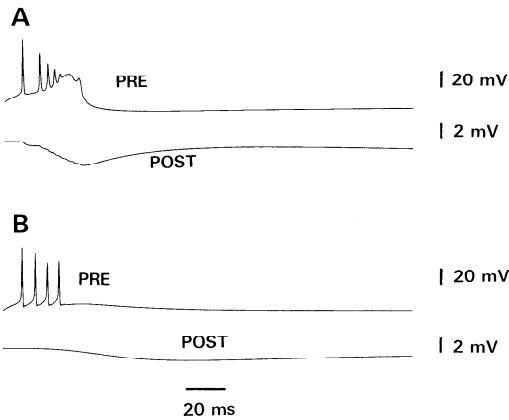
B

PRE | 20 mV

POST | 2 mV

20 ms

FIG. 2. Inhibition in the model. In each case, an inhibitory neuron (i-cell) is connected to an excitatory neuron. *A*: bursting i-cell (*upper trace*) is stimulated with a 0.8-nA 10-ms current. The resulting "fast" IPSP (at the soma) is shown *below*, where the fast inhibitory conductance parameter is 6 nS. *B*: repetitively firing i-cell is stimulated with a 0.8-nA 30-ms current. This generates a "slow" IPSP (below).

pend on the relative positions of the cells (see *Axonal conduction delays* below). A signal from an e-cell arriving at a postsynaptic neuron (either an e-cell or an i-cell) produces a total excitatory synaptic conductance in nanosiemens of $c_e t e^{-t/3}$ across four dendritic compartments, i.e., the conductance follows an α-function time course with time constant 3 ms. We denote c_e the "excitatory conductance parameter." The excitatory conductance develops across four dendritic compartments (as in Ref. 46) and is distributed to each compartment in proportion to its surface area. The EPSP reversal potential is 60 mV positive to resting potential. If the postsynaptic cell is an i-cell, then c_e is 10 nS. Otherwise, the value of c_e depends on the simulation and will be specified in the RESULTS. The value of c_e corresponds to conductance developed in the dendrites. The conductance that would be measured at the soma would be about fivefold smaller (see Ref. 44).

An input from a bursting i-cell is distributed to the soma and one compartment on either side of the soma (i.e., 1 compartment in the apical direction and 1 in the basilar direction), the compartmental conductance being proportional to surface area. The total conductance c is governed by the equation

$$\frac{dc}{dt} = c_{if} \times \left(I_2(T) - \frac{c}{7} \right)$$

where $I_2(t) = 1$ when $0 \le t \le 2$ ms and $I_2(t) = 0$ when $t > 2$ ms. Thus the time constant of decay is 7 ms. [Compare this with the time constant 8.3 ms

for decay of inhibitory postsynaptic currents in CA1 cells at 32° (6) and the decay time constant of 20 ms in cultured hippocampal neurons at 21–24° (36).] The value of c_{if}, the "fast inhibitory conductance parameter," depends on the particular simulation.

An input from a repetitively firing i-cell is distributed to the same dendritic compartments as excitatory inputs. At time t after a slow input arrives, the conductance c is given by a differential equation

$$\frac{dc}{dt} = k \times \left(I_{40}(t) - \frac{c}{100} \right)$$

where $I_{40}(t) = 1$ when $0 \le t \le 40$ ms and $I_{40}(t) = 0$ when $t > 40$ ms, and k is a constant (0.04 nS). Thus the conductance grows at a constant rate for 40 ms, while decaying with time constant 100 ms during the growth phase and afterward. With this k, the peak hyperpolariation produced at the soma of an e-cell by a train of four action potentials was −1.6 mV, 80 ms after the first presynaptic action potential (Fig. 2).

The reversal potential for both types of IPSP is 15 mV negative to resting potential. (The reversal potential for potassium currents in our single cell model is also 15 mV negative to resting potential.)

Synaptic inputs of a given type, arriving at different times and from different cells onto a particular postsynaptic cell, add linearly.

Synaptic connectivity

Every cell (either an e-cell or i-cell) has some probability of connecting to every other cell. The probability depends on the pre- and postsynaptic cell types, but not on their relative positions. [Data of Tamamaki et al. (37), based on horseradish peroxidase fills of pyramidal cell axons, suggest that the axon branches widely, without clear evidence of local structure.] Thus the statistical properties of the network topology depend on four parameters; P_{ee} (probability for one e-cell to contact another e-cell), P_{ei} (probability for an e-cell to contact an i-cell), P_{ie}, and P_{ii}. Although precise data for these probabilities are not available, estimates may be made from dual intracellular recordings. We do know that all recorded pyramidal neurons receive some inhibitory input. Furthermore, IPSPs occur in i-cells, spontaneously or after afferent stimulation, so that P_{ii} is not 0. Symmetric synapses are also found by electron microscopy on the somas of basket cells.

The particular values we used were, for 1,020 cell networks: $P_{ee} = 0.015$, $P_{ei} = 0.05$, $P_{ie} = 0.45$, $P_{ii} = 0.25$; for 520 cell networks: $P_{ee} = 0.03$, $P_{ei} = 0.1$, $P_{ie} = 0.8$, $P_{ii} = 0.8$. Some relevant experiments showing the reasonableness of these parameter choices are as follows. Miles and Wong (26) estimated P_{ee} as between 0.01 and 0.02 by dual

intracellular recording. With $P_{ee} = 0.015$ in the 1,020-cell network, the probability of at least one disynaptic excitatory path from one e-cell to another is $1 - (1 - 0.015^2)^{1,000} = 0.20$. When inhibition was suppressed, polysynaptic EPSPs were detected in $41/241 = 17\%$ of simultaneous recordings from pairs of bursting neurons (28). With our value of P_{ei} and P_{ie}, the probability that one e-cell disynaptically inhibits another e-cell is $1 - (1 - 0.05 \times 0.45)^{20} = 0.37$. The experimental value is 0.3 (Ref. 25, and R. Miles and R. K. S. Wong, unpublished observations). We expect the experimental value to be somewhat less than the value in the model network, since the numbers P_{ee}, P_{ei}, etc., define the number of topological paths between cells, whereas physiological measurements detect only pathways that are functionally effective, i.e., where spikes are actually transmitted faithfully across intervening synapses. With $P_{ie} = 0.45$ in the 1,020-cell network, 1 i-cell contacts 450 e-cells; Andersen, Eccles, and Løyning (4) estimated that one basket cell contacts 200–500 cells.

We also performed control runs with $P_{ii} = 0$ if it appeared disinhibition (i.e., inhibition of inhibitory neurons) was influencing the results, and control runs with $P_{ei} = 1$, so that every e-cell contacted every i-cell. The latter control run would work only with low levels of population activity, i.e., where inhibition is "strong"; otherwise, each inhibitory cell could be simultaneously stimulated by hundreds of e-cells, and, with the value of c_e used for e-i connections, our integration algorithm became unstable. This could be overcome by decreasing c_e, but that led to unphysiological results in that e-i spike latency became too long, or eventually a burst in an e-cell would not elicit a spike at all in a connected i-cell; this latter situation seems to be contradicted by physiological experiments showing that disynaptic inhibition from one e-cell to another can be both quite faithful (single presynaptic spikes frequently eliciting unitary IPSPs) and of latency as short as 3 ms (25). (An experiment that would help to define P_{ei} better would be to measure the unitary excitatory conductance in an i-cell and to compare that with the conductance developing in a PTX-induced synchronized burst.)

Axonal conduction delays

Experiments on the propagation of PTX-induced synchronized bursts across CA3 have suggested that axonal conduction along local collaterals is very slow in the hippocampus and, further, that propagation does not occur at the same velocity in either direction (20). Velocities have been estimated of 0.1 M/s going from CA2 toward CA4, and 0.2 M/s from CA4 toward CA2 (20). We incorporated these delays in our model as fol-

lows. Consider an e-cell A at location (k_1, l_1) and another, cell B, at (k_2, l_2). The time in milliseconds for a signal to travel from A to B is $0.2(l_2 - l_1)$ if $l_2 \geq l_1$ and is $0.1(l_1 - l_2)$ if $l_1 > l_2$. If a cell diameter is 20 μm, this corresponds to the experimentally estimated conduction velocities. In the case that A is an i-cell, the delay time is $0.02|l_1 - l_2|$. We used a shorter delay time in this case because of data suggesting that local axons of neocortical cells with smooth dendrites (presumably i-cells) are myelinated (17). The conduction velocity of i-cell axons in hippocampus is not known.

Initial conditions

All of the neurons begin in their resting state, i.e., at resting potential and with membrane state variables at or near their equilibrium values for resting potential (e.g., state variable $m = 0$, $h = 1$, etc.). The stimulus was a current of 2 nA for 10 ms injected into either one or four e-cells.

Features omitted from the model

We performed some simulations that included field interactions, but for the question of interest here, these interactions appeared not to be relevant. Since inclusion of field interactions greatly increased computing requirements, most simulations did not include them.

Computing requirements

Programs were written in Fortran and run on an IBM 3084 and an IBM 3090. Simulations of 200 ms of activity with 1,000 cells typically took ~35 min of CPU time on the 3090 with 6 Mbytes of virtual memory.

RESULTS

In Fig. 3, we illustrate the response of a 1,020 cell network to a burst in a single e-cell (the "initiating cell"), using three different levels of c_{if}, the parameter determining the strength of "fast" inhibition. The c_e was 4 nS, large enough to allow propagation of bursting from e-cell to e-cell in the absence of inhibition, a notion consistent with previous experiments and simulations. In each case, we plot, as a function of time, the number of e-cells and of i-cells depolarized above some threshold value (20 mV, the value corresponding to that when the cell can generate an output), the somatic potential of a particular e-cell (number 213), and the differing synaptic conductances to cell 213. The shortest e-cell path from the initiating cell to 213 involves one intermediate cell. Several points are worthy of note in Fig. 3. First, even at a "strong" level of inhibition (Fig. 3A), a num-
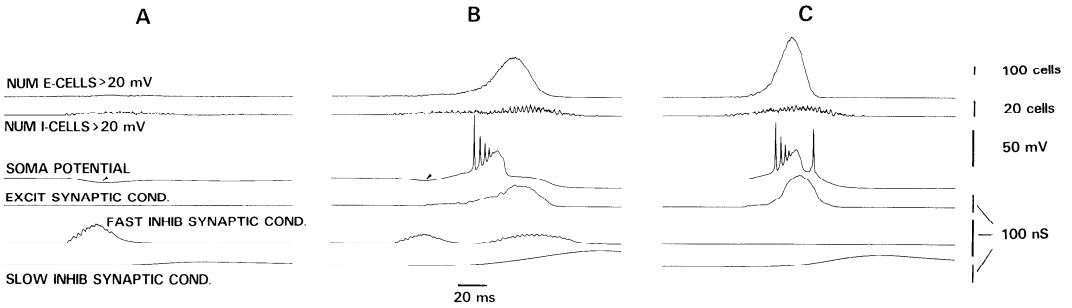
FIG. 3.   Response of 1,020 cell model [1,000 excitatory neurons (e-cells), 20 inhibitory neurons (i-cells)] to a current-induced burst in 1 cell, for 3 values of c_{if}, the fast inhibitory conductance parameter. Shown in each case are, from above, the number of e-cells depolarized above 20 mV (threshold for sending an output), the number of i-cells depolarized above 20 mV, the somatic potential of a particular cell (number 213, disynaptically removed from the initiating cell), the excitatory conductance input to cell 213, the "fast" inhibitory conductance input to cell 213, and the slow inhibitory input to cell 213. In A, c_{if} is 8 nS. There is low-level e-cell activity, not enough to deliver any excitation to cell 213, but enough so that it receives both types of inhibition. (*Arrow* indicates IPSP.) In B, c_{if} is 4 nS. A broad, incomplete synchronized burst develops. Cell 213 shows an initial IPSP (*arrow*), followed by a burst, followed by a synaptically and intrinsically generated afterhyperpolarization. In C, c_{if} is 0. A large synchronized burst occurs. Cell 213 receives a very large excitatory input [peaking at 180 nS—the conductance measured at the soma during this input would be ∼35 nS (44), so that this value is quite reasonable (16)]. The slow IPSP contributes to the afterhyperpolarization, but does not develop rapidly enough to prevent synchronization.

ber of e-cells fire, including seven out of the eight e-cells connected to the initiating cell. A maximum of 21 cells reach 20 mV or above at once. Cell 213, however, shows only an IPSP (with both fast and slow components, something not apparent from the voltage record). Thus, in this model system, inhibition is not able to suppress totally some unavoidable firing as a consequence of bursting in one cell. The synaptic responses of 15 e-cells (randomly selected) in this simulation were as follows: pure EPSP, 1; pure IPSP, 3; EPSP-IPSP sequence, 3; IPSP-EPSP sequence, 1; IPSP-EPSP-IPSP, 6; firing, none. At an "intermediate" level of inhibition, the population becomes partially synchronized, with a greatly increased amount of cell firing (Fig. 3B). Cell 213 now bursts, but there is an IPSP leading the burst. The response of cell 213 reflects the complex interaction of its intrinsic properties with the three types of synaptic input impinging on it (excitation and two types of inhibition). This kind of cellular behavior is reminiscent of a neuron in a high-K$^+$ medium illustrated by Rutecki et al. (32) and of neurons in the intermediate zone of the inhibitory surround of an in vivo penicillin hippocampal focus (7, 8, 41). In 15 e-cells plotted in this simulation, there was a clear leading IPSP in four of them. Finally, with fast inhibition totally

"blocked" (Fig. 3C, c_{if} = 0), all e-cells fire. [The ability of a burst in a single cell to induce synchronized activity in a population of neurons in the presence of PTX has been shown experimentally (24).] The latency to the peak of the e-cell firing curve is reduced, compared with Fig. 3B, its peak is higher and the curve is narrower. Cell 213 shows no leading hyperpolarization, its excitatory synaptic input begins sooner and is larger, and it fires an extra spike compared with Fig. 3B. Slow inhibition peaks after the synchronized burst is virtually over, and so it does not prevent the initial synchronized burst. This is not to say that the slow IPSP is irrelevant in terms of whether afterdischarges develop, a matter not pursued here (10, 29). It is interesting that with a reduced degree of e-cell to e-cell connectivity (P_{ee} = 0.005 instead of the usual 0.015), slow inhibition markedly reduces the degree of synchronization elicited by stimulating one cell (not shown).

Figure 4 illustrates the changing responses of another e-cell (number 201) in the same network for a series of different fast inhibitory strengths. The shortest path from the initiating cell to cell 201 is via two intermediate cells. Figure 4Aa is from the same run as Fig. 3A, whereas Fig. 4Ad is from the same run as Fig. 3B. Cell 201 shows the sequence of responses mentioned in the INTRODUC-

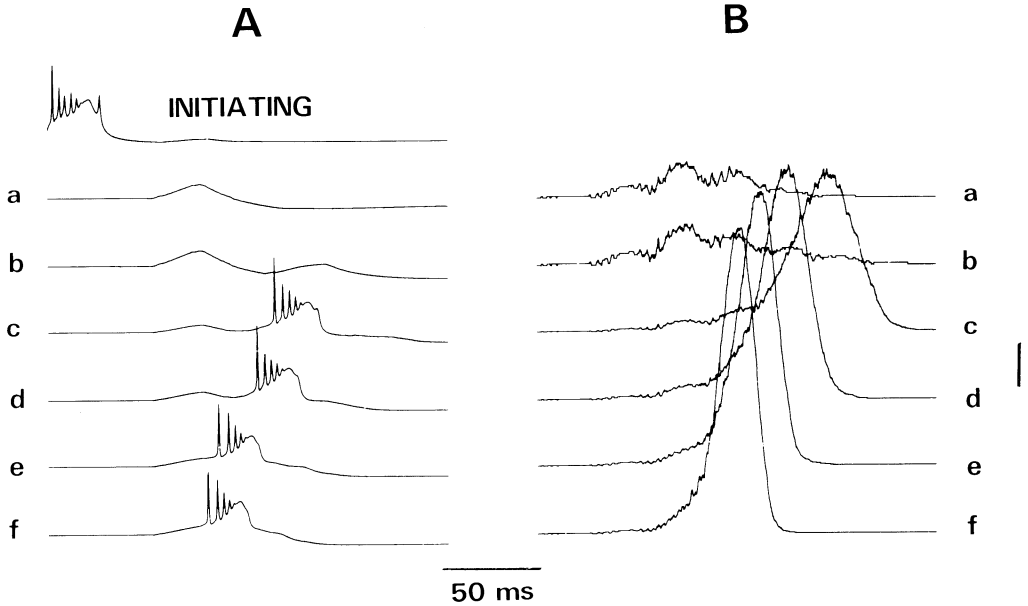**A**   **B**

INITIATING

50 ms

FIG. 4.   The network is the same as in Fig. 3, again with a stimulus to 1 cell ("initiating"). Six runs were performed, with successively decreasing levels of fast inhibition, in order to show, in A, the responses of a particular cell (number 201, trisynaptically removed from the initiating cell), and, in B, the simultaneous population response (i.e., the number of excitatory neurons depolarized above 20 mV). *Abscissa* is time. The initiating cell plot is from simulation b. (With lower values of fast inhibition, the burst in the initiating cell is followed by a large EPSP or by a second burst, as also occurs experimentally.) a: the fast inhibitory conductance parameter (c_{if}) = 8 nS. Cell 201 shows a single EPSP (since only one of its precursors bursts—not shown). The population response is limited. b: c_{if} = 7 nS. A double EPSP occurs, since 2 precursors to cell 201 burst, at different times (not shown). The initial part of the population response is almost identical to a, but a few more cells burst toward the end. c: c_{if} = 5 nS. A qualitative change in behavior occurs: the population response increases dramatically (Bc), all precursors to 201 burst (not shown), cell 201 shows an EPSP followed by a burst (Ac). d–f: c_{if} = 4, 3, and 2 nS, respectively. Synchronization becomes larger, sharper, and of shorter latency (B). The burst in cell 201 and the initial EPSP decrease in latency and also merge. Calibrations: A: 50 mV for initiating and c–f, 25 mV for a and b; B: 25 cells firing for a and b, 100 cells firing for c–f.

TION, that has been observed in an actual neuron: an EPSP, a pair of EPSPs, an EPSP followed by a burst, and EPSP merging into a burst of decreasing latency (28). Figure $4B$ shows that these changing responses in an individual cell correspond to changes in the e-cell firing curve of the population: increasing amplitude, shortening latency, and sharpening. Furthermore, we were able to correlate the response of cell 201 with the behavior of all of its 14 input e-cells. Thus, in the run of Fig. 4Aa, exactly one excitatory precursor fires a burst, whereas the others do not fire at all (not shown). In Fig. 4Ab, two precursors burst, but at different times, thus generating temporally separated EPSPs. There is a "jump" in moving to Fig. 4Ac, in that now all 14 precursor cells burst (not shown). Note that cell 201, unlike cell 213, never shows a leading IPSP, so that with in-

hibition present, different cells respond to a given stimulus in different ways. In the kind of situation analyzed here, the topological details of the network really do make a difference.

This picture is consistent with the notion of inhibitory blockade allowing propagation along new paths. In addition, as paths open up, particular neurons become excited more and more strongly, shortening their latency to firing, this in turn having additional consequences further "downstream."

We next examine the degree of synchronization (measured as the peak of the e-cell firing curve) as a function of c_{if}, the parameter determining the strength of fast inhibition (Fig. 5). The value of c_e used in the runs generating this figure was as in previous figures (4 nS). The curve of Fig. 5 has a sudden change of slope at the point marked "Y". In
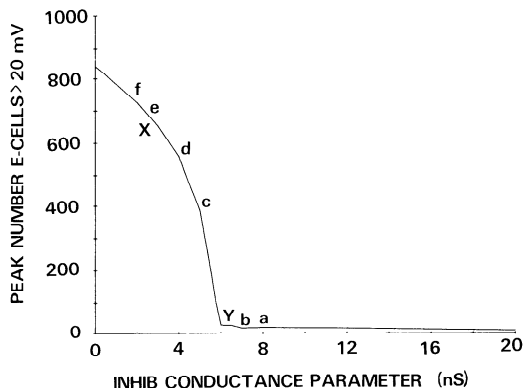
FIG. 5.   Curve of the peak number of excitatory neurons (e-cells) depolarized above 20 mV vs. the fast inhibitory conductance parameter (c_{if}). Same network as in Fig. 3 and 4. This curve uses data from the runs generating Figs. 3 and 4 (with corresponding runs from Fig. 4 marked on the curve), together with other runs. The stimulus is in each case to 1 cell. Note that there is at least some small degree of induced bursting at all levels of inhibition, but there is a qualitative change in behavior at *point Y* (c_{if} = 6 nS, midway between runs b and c of Fig. 4). E-cell-to-e-cell propagation occurs in a 3-cell network when c_{if} = 2.4 nS, marked on the *curve* by "X" (see text).

order to interpret this, we performed a series of simulations with a three-cell network in which e-cell A is excited by e-cell B (with c_e as in Fig. 5) and simultaneously inhibited by bursting i-cell C (with multiple values of c_{if} used, corresponding to the values in Fig. 5). Cells B and C were induced to burst simultaneously, and we asked: for what values of c_{if} would bursting appear in cell A? This value of c_{if} corresponds naively to a level of inhibition at which propagation of bursting from e-cell to e-cell can just occur. (We say naively, because details of timing and multicellular inputs are ignored in this analysis.) We expected that cell-to-cell propagation would occur at a level of inhibition corresponding to point Y in Fig. 5, but, in fact, propagation occurs only at significantly lower levels of inhibition, e.g., at point X. To put this another way, some degree of synchronization can take place with a degree of inhibition that apparently ought to prevent synchronization. However, two mechanisms work to allow this kind of partial synchronization. First, we found neurons (such as cell 201) where the excitatory input arrives before inhibition, simply because of delays in the dif-

ferent circuits. Second, comparing in detail the runs of Fig. 4*A*b and 4*A*c, we were able to find cells receiving multiple (3 or 4) bursting inputs, rather than only one, so that at one level of inhibition three bursting precursors could not induce bursting into a postsynaptic neuron, but at another level of inhibition three bursting precursors were effective. In short, multicellular interactions are taking place, and the above three-cell network is not adequate to make quantitative predictions in this case (see, however, below).

In Fig. 6, using a 520 cell network, we illustrate the peak of the e-cell firing curve as a function of c_e, at two levels of inhibition: c_{if} = 0 and 7 nS (7 nS is the value used in Fig. 4*A*b). We used the smaller network because of the large number of runs required to produce these curves. When c_{if} = 0, there is an abrupt rise in the peak number of cells firing as c_e becomes large enough for cell-to-cell propagation of bursting (point X in Fig. 6). A larger value of c_e is necessary for bursting propagation when inhibition is present (point Y in Fig. 6). The rise in peak number of cells firing is not as abrupt as when there is no inhibition, since some e-cells are inhibited by several i-cells. Nevertheless, if the excit-
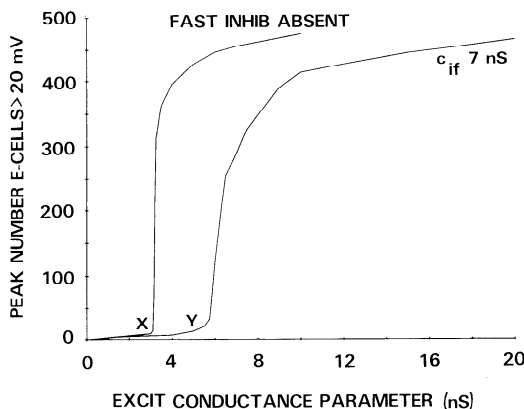

FIG. 6.   Plots of peak number of excitatory neurons (e-cells) depolarized above 20 mV vs. c_e, the excitatory conductance parameter, at 2 values of c_{if} (0 and 7 nS). Data from a network of 500 e-cells and 20 i-cells, stimulus to 4 e-cells. When c_{if} = 0, there is a virtual corner in the *curve* at X, corresponding to a value of c_e where propagation can occur from one e-cell to another. When c_{if} = 7 nS, propagation in a 3-cell network occurs at a c_e value corresponding to Y, near (but slightly less than) the point of sudden, steep rise in the *curve*.

atory synapses are sufficiently powerful, the peak number of e-cells firing in the presence of rather strong fast inhibition is similar to the peak number firing in the absence of fast inhibition. This was even the case with larger values of c_{if} than 7 nS. For example, with c_{if} = 15 nS, a peak of 832 cells fired together with c_e = 15 nS (in a network of 1,020 cells).

DISCUSSION

The main insights provided by these simulations concern the effects of inhibition on a system of neurons that are mutually interconnected by strong, but sparse, excitatory synapses. The outstanding features of the inhibitory system we have used are these: i-cells are of different physiological types and produce different time courses of inhibition; the number of e-cells any particular i-cell "sees" is a relatively small fraction of the population (so, given that there are few i-cells compared with e-cells, some e-cells do not contact any i-cells in our model); the output of each i-cell is widely divergent, so that virtually all e-cells are inhibited by at least one (usually more than 1) i-cell. With these features, the i-cell subsystem is able to prevent the unbounded propagating growth resulting from a single cell bursting that would occur in the absence of fast inhibition. Nevertheless, inhibition at any strength does not abolish all e-cell activity consequent upon one cell bursting. This occurs because 1) it takes variable amounts of time for inhibition to reach the followers of a given e-cell, and inhibition may arrive too late to prevent propagation; 2) with low levels of activity, some followers of an e-cell may not be inhibited at all, if the inhibitory precursors of a follower are not excited by the bursting e-cells. Only when sufficiently many e-cells burst do all or most of the i-cells fire.

Our simulations also provide some insight into the richness of this system. Thus, at low and intermediate levels of inhibition, different e-cells respond quite differently to a burst in a given e-cell, and to understand the differing response one must take into account much of the network topology, i.e., all the paths (up to some length) from the bursting cell to the two different e-cells. Even our

model represents a simplified case, however, since the cells begin at rest. In the actual brain, ongoing activity and extrinsic inputs will alter the states of various cells along the paths between given cells, making an analysis that much more difficult. One can imagine propagation being "guided" in different directions depending on such inputs. We comment that the model manifests this richness because we were able to simulate individual neurons with some realism and because the model contains over 1,000 cells (of the same order of magnitude as the actual CA3 region in the slice) with a plausible degree of connectivity; this in turn allows a diversity of paths between different neurons.

Since inhibition in the hippocampus is labile (23, 39, 53), the qualitative behavior of regions of CA3 (in terms of varying population responses to bursting in a particular subset of neurons) may vary with time. This would be especially interesting if the level of inhibition fluctuates around point Y in Fig. 5, implying that small changes in inhibitory synaptic efficacy could lead to large changes in population response.

While we analyzed in detail the effects of blockade of fast, convulsant-sensitive inhibition, based on experimental data, we did not attempt a similar detailed analysis of the effects of blockade of slow inhibition. One reason is that, in the absence of data using a specific blocker of slow inhibition, we did not have experiments to guide us. We did observe that under the conditions of our model, slow inhibition does not prevent the development of a single synchronized discharge, unless the excitatory connectivity is low (see RESULTS). This observation may be relevant to epileptogenesis in neocortex, where excitatory synaptic interconnections may not be as powerful as in hippocampus. Slow inhibition has marked effects on the spontaneous behavior of our model (45).

These simulations have relevance to clinical epilepsy. Synchronized or partly synchronized bursts occur in situations where inhibition is probably not totally blocked (54). It is apparent that this behavior is expected if there is some propagation of bursting from e-cell to e-cell in spite of inhibition. The simulations reported here indicate that this will happen if excitatory synapses are powerful

cnough, with the resulting synchronized event perhaps being "sloppy" (i.e., of small amplitude, broadened in time, of long latency). If either excitatory or inhibitory transmission fluctuates, one can imagine that failures of population synchronized bursts would also occur. We expect that partial synchronization would also be favored by factors that render e-cells more excitable, since this would in turn favor propagation of bursting from cell to cell. We did not analyze this particular issue in detail.

For the further development of these results, two main areas demand attention. First, it would be helpful to pin down the anatomical and physiological parameters more precisely. How many e-cells contact a given i-cell? How are the connections distributed in space? Is it true that not all e-cells contact any i-cell? Second, it would be helpful to have theoretical tools to aid the understanding of realistic neuronal networks such as simulated here. The problem is complicated because *1)* the individual neurons are complex machines with large numbers of inputs and subtle dynamics, having many overlapping time scales (i.e., single action potentials lasting 1 or 2 ms up to K^+ currents lasting seconds, with both longer and shorter

time constants conceivable); *2)* there is a large number of cells, and the details of the individual connections matter, at least for certain issues. Only when there is a firm understanding of the dynamics of realistic neuronal models such as this, grounded in physiological experiments, will we have a proper base for thinking about plasticity in neuronal systems.

In the next paper, we show that our model, if allowed to run for several seconds, develops—in the presence of inhibition—unexpected periodic behaviors of a type observed in some cortical slice systems. As inhibition is blocked, the model generates sequences of partially synchronized bursts followed by a "major" synchronized burst, again as observed experimentally in hippocampal slices bathed in low concentrations of penicillin.

REFERENCES

1. ADAMS, P. R., BROWN, D. A., AND HALLIWELL, J. V. Cholinergic regulation of M-current in hippocampal cells. *J. Physiol. Lond.* 317: 29P–30P, 1981.
2. ALGER, B. E. Characteristics of a slow hyperpolarizing synaptic potential in rat hippocampal pyramidal cells in vitro. *J. Neurophysiol.* 52: 892–910, 1984.
3. ALGER, B. E. AND NICOLL, R. A. Epileptiform burst afterhyperpolarization: calcium-dependent potassium potential in hippocampal CA1 pyramidal cells. *Science Wash. DC* 210: 1122–1124, 1980.
4. ANDERSEN, P., ECCLES, J. C., AND LØYNING, Y. Recurrent inhibition in the hippocampus with identification of the inhibitory cell and its synapses. *Nature Lond.* 198: 540–542, 1963.
5. BUCKLE, P. J. AND HAAS, H. L. Enhancement of synaptic transmission by 4-aminopyridine in hippocampal slices of the rat. *J. Physiol. Lond.* 326: 109–122, 1982.
6. COLLINGRIDGE, G. L., GAGE, P. W., AND ROBERTSON, B. (1984) Inhibitory post-synaptic currents in rat hippocampal CA1 neurones. *J. Physiol. Lond.* 356: 551–564, 1984.
7. DICHTER, M. AND SPENCER, W. A. Penicillin-in-

duced interictal discharges from the cat hippocampus. I. Characteristics and topographical features. *J. Neurophysiol.* 32: 649–662, 1969.
8. DICHTER, M. AND SPENCER, W. A. Penicillin-induced interictal discharges from the cat hippocampus. II. Mechanisms underlying origin and restriction. *J. Neurophysiol.* 32: 663–687, 1969.
9. DINGLEDINE, R. AND GJERSTAD, L. Reduced inhibition during epileptiform activity in the in vitro hippocampal slice. *J. Physiol. Lond.* 305: 297–313, 1980.
10. GALVAN, M., GRAFE, P., AND TEN BRUGGENCATE, G. Convulsant actions of 4-aminopyridine on the guinea-pig olfactory cortex slice. *Brain Res.* 241: 75–86, 1982.
11. GAMRANI, H., ONTENIENTE, B., SEGUELA, P., GEFFARD, M., AND CALAS, A. Gamma-aminobutyric acid-immunoreactivity in the rat hippocampus. A light and electron microscopic study with anti-GABA antibodies. *Brain Res.* 364: 30–38, 1986.
12. HABLITZ, J. J. Effects of intracellular injections of chloride and EGTA on postepileptiform burst hyperpolarizations in hippocampal neurons. *Neurosci. Lett.* 22: 159–163, 1981.

13. HALLIWELL, J. V. AND ADAMS, P. R. Voltage-clamp analysis of muscarinic excitation in hippocampal neurons. *Brain Res.* 250: 71–92, 1982.

14. HOCH, D. B. AND DINGLEDINE, R. GABAergic neurons in rat hippocampal culture. *Dev. Brain Res.* 25: 53–64, 1986.

15. HOTSON, J. R. AND PRINCE, D. A. A calcium-activated hyperpolarization follows repetitive firing in hippocampal neurons. *J. Neurophysiol.* 43: 409–419, 1980.

16. JOHNSTON, D. AND BROWN, T. H. Giant synaptic potential hypothesis for epileptiform activity. *Science Wash. DC* 211: 294–297, 1981.

17. JONES, E. G. Identification and classification of intrinsic circuit elements in the neocortex. In: *Dynamic Aspects of Neocortical Function,* edited by G. M. Edelman, W. E. Gall, and W. M. Cowan. New York: Wiley, 1984, p. 7–40.

18. KNOWLES, W. D., SCHNEIDERMAN, J. H., WHEAL, H. V., STAFSTROM, C. E., AND SCHWARTZKROIN, P. A. Hyperpolarizing potentials in guinea pig hippocampal CA3 neurons. *Cell. Mol. Neurobiol.* 4: 207–230, 1984.

19. KNOWLES, W. D. AND SCHWARTZKROIN, P. A. Local circuit synaptic interactions in hippocampal brain slices. *J. Neurosci.* 1: 318–322, 1981.

20. KNOWLES, W. D., TRAUB, R. D., AND STROWBRIDGE, B. W. The initiation and spread of epileptiform bursts in the in vitro hippocampal slice. *Neuroscience* 21: 441–455, 1987.

21. KORN, S. J., GIACCHINO, J. L., CHAMBERLIN, N. L., AND DINGLEDINE, R. Epileptiform burst activity induced by potassium in the hippocampus and its regulation by GABA-mediated inhibition. *J. Neurophysiol.* 57: 325–340, 1987.

22. MACVICAR, B. A. AND DUDEK, F. E. Local synaptic circuits in rat hippocampus: interactions between pyramidal cells. *Brain Res.* 184: 220–223, 1980.

23. MCCARREN, M. AND ALGER, B. E. Use-dependent depression of IPSPs in rat hippocampal pyramidal cells in vitro. *J. Neurophysiol.* 53: 557–571, 1985.

24. MILES, R. AND WONG, R. K. S. Single neurones can influence synchronized population discharge in the CA3 region of the guinea pig hippocampus. *Nature Lond.* 306: 371–373, 1983.

25. MILES, R. AND WONG, R. K. S. Unitary inhibitory synaptic potentials in the guinea-pig hippocampus in vitro. *J. Physiol. Lond.* 356: 97–113, 1984.

26. MILES, R. AND WONG, R. K. S. Excitatory synaptic interactions between CA3 neurones in the guinea pig hippocampus. *J. Physiol. Lond.* 373: 397–418, 1986.

27. MILES, R. AND WONG, R. K. S. Excitatory synaptic connections between guinea pig CA3 hippocampal cells are revealed when synaptic inhibition is suppressed in vitro. *J. Physiol. Lond.* 372: 14P, 1986.

28. MILES, R. AND WONG, R. K. S. Inhibitory control of local excitatory synaptic circuits in the guinea pig hippocampus. *J. Physiol. Lond.* 388: 611–629, 1987.

29. MILES, R., WONG, R. K. S., AND TRAUB, R. D. Synchronized afterdischarges in the hippocampus: contribution of local synaptic interaction. *Neuroscience* 12: 1179–1189, 1984.

30. NEWBERRY, N. R. AND NICOLL, R. A. A bicuculline-resistant inhibitory postsynaptic potential in rat hippocampal pyramidal cells in vitro. *J. Physiol. Lond.* 348: 239–254, 1984.

31. RIBAK, C. E., VAUGHN, J. E., AND SAITO, K. Immunocytochemical localization of glutamic acid decarboxylase in neuronal somata following colchicine inhibition of axonal transport. *Brain Res.* 140: 315–332, 1978.

32. RUTECKI, P. A., LEBEDA, F. J., AND JOHNSTON, D. Epileptiform activity induced by changes in extracellular potassium in hippocampus. *J. Neurophysiol.* 54: 1363–1374, 1985.

33. RUTECKI, P. A., LEBEDA, F. J., AND JOHNSTON, D. 4-Aminopyridine produces epileptiform activity in hippocampus and enhances synaptic excitation and inhibition. *J. Neurophysiol.* 57: 1911–1924, 1987.

34. SCHWARTZKROIN, P. A. AND MATHERS, L. H. Physiological and morphological identification of a nonpyramidal hippocampal cell type. *Brain Res.* 137: 1–10, 1978.

35. SCHWARTZKROIN, P. A. AND STAFSTROM, C. E. Effects of EGTA on the calcium-activated afterhyperpolarization in hippocampal CA3 cells. *Science Wash. DC* 210: 1125–1126, 1980.

36. SEGAL, M. AND BARKER, J. L. Rat hippocampal neurons in culture: voltage-clamp analysis of inhibitory synaptic connections. *J. Neurophysiol.* 52: 469–487, 1984.

37. TAMAMAKI, N., WATANABE, K., AND NOJYO, Y. A whole image of the hippocampal pyramidal neuron revealed by intracellular pressure-injection of horseradish peroxidase. *Brain Res.* 307: 336–340, 1984.

38. THALMANN, R. H. Reversal properties of an EGTA-resistant late hyperpolarization that follows synaptic stimulation in hippocampal neurons. *Neurosci. Lett.* 46: 103–108, 1984.

39. THALMANN, R. H. AND HERSHKOWITZ, N. Some factors that influence the decrement in the response to GABA during its continuous iontophoretic application to hippocampal neurons. *Brain Res.* 342: 219–233, 1985.

40. TRAUB, R. D. Simulation of intrinsic bursting in CA3 hippocampal neurons. *Neuroscience* 7: 1233–1242, 1982.

41. TRAUB, R. D. Cellular mechanisms underlying the inhibitory surround of penicillin epileptogenic foci. *Brain Res.* 261: 277–284, 1983.

42. TRAUB, R. D., DUDEK, F. E., SNOW, R. W., AND KNOWLES, W. D. Computer simulations indicate that electrical field effects contribute to the shape of the epileptiform field potential. *Neuroscience* 15: 947–958, 1985.

43. TRAUB, R. D., KNOWLES, W. D., MILES, R., AND WONG, R. K. S. Synchronized afterdischarges in the hippocampus: simulation studies of the cellular mechanism. *Neuroscience* 12: 1191–1200, 1984.

44. TRAUB, R. D., KNOWLES, W. D., MILES, R., AND WONG, R. K. S. Models of the cellular mechanism underlying propagation of epileptiform activity in the CA2-CA3 region of the hippocampal slice. *Neuroscience* 21: 457–470, 1987.

45. TRAUB, R. D., MILES, R., WONG, R. K. S., SCHULMAN, L. S., AND SCHNEIDERMAN, J. H. Models of synchronized hippocampal bursts in the presence of inhibition. II. Ongoing spontaneous population events. *J Neurophysiol.* 58: 752–764, 1987.

46. TRAUB, R. D. AND WONG, R. K. S. Cellular mechanism of neuronal synchronization in epilepsy. *Science Wash. DC* 216: 745–747, 1982.

47. TRAYNELIS, S. F. AND DINGLEDINE, R. Prolonged seizure-like discharges in hippocampal neurons in vitro are triggered by spontaneous interictal bursts originating in the CA3 region. *Soc. Neurosci. Abstr.* 12: 74, 1986.

48. TURNER, D. A. AND SCHWARTZKROIN, P. A. Steady-state electrotonic analysis of intracellularly stained hippocampal neurons. *J. Neurophysiol.* 44: 184–199, 1980.

49. VOSKUYL, R. A. AND ALBUS, H. Spontaneous epileptiform discharges in hippocampal slices induced by 4-aminopyridine. *Brain Res.* 342: 54–66, 1985.

50. WONG, R. K. S. AND PRINCE, D. S. Dendritic mechanism underlying penicillin-induced epileptiform activity. *Science Wash. DC* 204: 1228–1231, 1979.

51. WONG, R. K. S. AND PRINCE, D. A. Afterpotential generation in hippocampal pyramidal cells. *J. Neurophysiol.* 45: 86–97, 1981.

52. WONG, R. K. S., PRINCE, D. A., AND BASBAUM, A. I. Intradendritic recordings from hippocampal neurons. *Proc. Natl. Acad. Sci. USA* 76: 986–990, 1979.

53. WONG, R. K. S. AND WATKINS, D. J. Cellular factors influencing GABA response in hippocampal pyramidal cells. *J. Neurophysiol.* 48: 938–951, 1982.

54. WYLER, A. R., OJEMANN, G. A., AND WARD, A. A., JR. Neurons in human epileptic cortex: correlation between unit and EEG activity. *Ann. Neurol.* 11: 301–308, 1982.